

Synthesis and characterization of zeolite X obtained from kaolin for adsorption of Zn(II)

Ismael I.S.*

Faculty of Science, Suez Canal University, Suez, Egypt

* Corresponding author, E-mail: ismaelsayed@hotmail.com

Received May 15, 2009; accepted June 10, 2009

© Science Press and Institute of Geochemistry, CAS and Springer-Verlag Berlin Heidelberg 2010

Abstract This study deals with the synthesis and characterization of low-silica zeolite X, from calcined Kalabsha kaolin, for adsorption of Zn(II) ions from aqueous solution. The synthesis processes is performed under hydrothermal treatment in alkaline solutions. The obtained zeolite samples are characterized using X-ray diffraction, grain size distribution, surface area, and SEM. The critical molar ratios of both $\text{SiO}_2/\text{Al}_2\text{O}_3$ and $\text{K}_2\text{O}/\text{Na}_2\text{O}$ are about 2.9 and 0.16, respectively. Those ratios are needed to give individual low silica zeolite X in a minimum reaction time. The adsorption capacity of the synthesized products is determined by adsorption of Zn(II) ions from solution. The results suggest that the zeolite obtained could be converted to a beneficial product, which will be used in future as an ion exchanger in removing heavy metals from wastewaters.

Key words kaolin; low silica zeolite; hydrothermal treatment; $\text{SiO}_2/\text{Al}_2\text{O}_3$ - $\text{K}_2\text{O}/\text{Na}_2\text{O}$ -Zn(II) exchange capacity

1 Introduction

Zeolites are three-dimensional, crystalline compounds which are built from AlO_4 and SiO_4 tetrahedra (Rollman and Valyocisk, 1981). Low-silica zeolites with Al/Si ratio of 1:1, such as zeolite A, zeolite P and zeolite X, exhibit the highest ion exchange capacity. Zeolite has been widely applied to practical processes in various industrial fields as a desiccant, an adsorbent, a molecular sieve, an ion exchanger, a catalyst and as the traditional water-softening agent in detergents (Ichiura et al., 2001; Nah et al., 2006; Wang et al., 2006) Otherwise, low-silica zeolites may be used as precursors for the synthesis of aluminosilicate ceramics (Falamaki et al., 2006; Roque et al., 2006).

Zeolite is usually synthesized under hydrothermal conditions, from solutions of sodium aluminate, sodium silicate or sodium hydroxide (Dwyer, 1984; Chandrasekhar and Pramada, 2008; Jiménez et al., 2008). Such conditions are typical of those found in the Earth's crust where some zeolite is found naturally. Kaolin is an ideal raw material for synthesis of low-silica zeolite because the contents of SiO_2 and Al_2O_3 are relatively similar with each other. The most common products prepared from thermally activated kaolin (calcined kaolin) or metakaolin are zeolite A and zeolite P (Gualtieri et al., 1997; Hassan et al., 2002; Mirfendereski et al., 2006). Zeolite X is another

important product, which can be prepared from kaolin usually with additional silica sources (Elena et al., 1995; Akolekar et al., 1997; Chandrasekhar and Pramada, 1999). Low-silica zeolite X (LSX) is much more difficult to prepare, requiring careful control over the synthesis conditions (Coe et al., 1988; Basaldella and Tara 1995; Akolekar et al., 1997).

The hydrothermal reactions of thermally activated kaolin (calcined kaolin) and metakaolin with aqueous sodium hydroxide have been studied by Hassan et al. (2002). Under their conditions, the major products of reaction of thermal activated kaolin (calcined kaolin) or metakaolin were zeolite A, and co-crystallization zeolite A+P. The authors proposed a mechanism in which the thermal activated kaolin (calcined kaoline) and metakaolin was dissolved in alkali to form a gel that was the direct precursor of zeolite A, and/or zeolite A+P. At synthesizing zeolite X, an increase of the aluminum content in its network (meaning use of a very low silica concentration) occurs, this led to cocrystallization of zeolite A, to avoid this cocrystallization, a low crystallization temperature together with seeding solution (Tatic and Drzaj, 1985) or the partial replacement of sodium ion by potassium ion in the formulation of the initial reaction mixture takes place (Coe et al., 1988). The aim of the study is to synthesize and characterize zeolite X from the Kalabsha kaolin for Zn(II) adsorption.

2 Materials and experimental techniques

2.1 Materials

The Wadi Kalabsha kaolin-type clay from the southwest of Aswan (Egypt) was chosen as the raw materials. This kaolin occurs at about 150 km southwest of Aswan. It is interbedded within the so-called Nubia sandstone of Upper Cretaceous age (El Badry et al., 1981; Shata, 1991). The Wadi Kalabsha kaolin occurs as both continuous and lenticular beds. The thickness ranges from a few centimeters to five meters. According to Said and Mansour (1971), the Nubia sandstone in Wadi Kalabsha falls into three members; Lower and Upper Sandstone Member, which enclose a Middle Kaolin Member. Although the main deposit lies within the Wadi Kalabsha Kaolin Member, some bands are found in the Upper Sandstone Member. The Wadi Kalabsha kaolin could be classified as a clastic deposit which was formed by the transportation of intensely weathered parent aluminous rocks and its deposition in a closed aqueous body.

2.2 Synthesis process

Thermally activated sample (dehydrated kaolin) was prepared by calcination of kaolin for 3 hours in air at 600°C. NaOH (89% E. Merck, D-6100 Darmstadt, F.R. Germany), commercial water glass [$\text{SiO}_2/\text{Na}_2\text{O}=3.18$ (W.W), density=1.36 g/mL], and distilled water were used for alkaline treatment. The hydrothermal synthesis of zeolite was carried out at autogenous pressure at 50°C in closed polypropylene containers with no stirring. During the development of the reaction, samples of the product were taken, to separate the liquid from solid. The solids obtained were washed with distilled water, dried in an oven at 100°C, and characterized by XRD. Electron micrographs were taken with Jeol JEM-7A electron microscope.

2.3 Adsorption process

These assays were carried out by mixing different dosages of synthesized products (zeolite A, zeolite A+X and zeolite X, respectively) in contact with 60 mL of Zn(II) solution (500 mg/L), which was prepared from the basic salt, zinc sulfate $\text{ZnSO}_4 \cdot 7\text{H}_2\text{O}$, at different pH. Zinc exchange was achieved in a thermostatic bath at 25°C under continuous agitation.

2.4 Characterization and analysis

The Kalabsha kaolin and zeolite obtained were characterized using Philips PW 1710 X-ray diffractometer, with $\text{CuK}\alpha$ radiation and operating at 40 kV

and 20 mA, and a Ni filter. The sample speed was two degrees per minute. The chemical composition of kaolin was determined using a Philips PW 1410 X-ray spectrometer. Differential thermal analysis of kaolin was performed using Netzsch simultaneous thermal analysis type STA 90 at the heating rate of 10°C/min. The zinc concentrations in the starting solution and filtered solution were measured using a Perkin-Elmer Analyst 100 atomic absorption spectrophotometer (AAS).

3 Results and discussion

The X-ray diffraction pattern (Fig. 1) of the original sample shows that the Kalabsha kaolin was composed mainly of kaolinite, quartz, and a minor amount of anatase. The Kalabsha kaolin exhibited two peaks in its DTA curve, an endothermic peak at about 608°C, associated with the loss of water from the structure hydroxyls and exothermic one at 998°C due to the formation of a new phase with spinel-like type structure. The chemical composition of the Kalabsha kaolin is listed in Table 1.

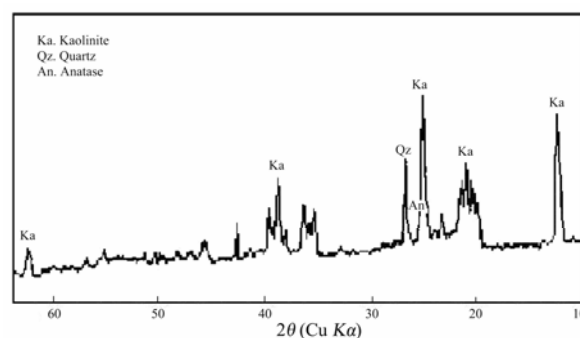


Fig. 1. X-ray diffraction of the Kalabsha kaolin.

Table 1. The chemical composition of the Kalabsha kaolin

Element oxide	%
SiO_2	46.35
Al_2O_3	31.50
Fe_2O_3	9.51
TiO_2	1.65
Na_2O	0.02
K_2O	0.08
CaO	1.21
MgO	0.13
Soluble salt	0.22

The reaction medium consists of solid phase (calcined kaolin) in contact with alkaline liquor. The hydrothermal treatment processes were performed at 50°C for one to five weeks, commercial water glass was used as an additional source when needed. The molar ratios, at the beginning of the reaction were:

$$\text{SiO}_2/\text{Al}_2\text{O}_3=1.5 \text{ to } 2.9$$

$$\text{K}_2\text{O}/\text{Na}_2\text{O}=0.05 \text{ to } 0.15$$

$$\text{H}_2\text{O}/(\text{K}_2\text{O}+\text{Na}_2\text{O})=20$$

Those ratios were chosen on the basis of previously cited data. It was reported that it is possible to obtain zeolite X (Basaldella and Tara, 1995; Elena et al., 1995), assuming that silica present as quartz remains unchanged during treatments.

(1) In the first course of reaction the K_2O/Na_2O ratio was fixed at 0.09 and the ratio of SiO_2/Al_2O_3 varied from 1.5 to 2.6 to 2.9.

(2) In the second course of reaction SiO_2/Al_2O_3 was fixed at 2.6 and K_2O/Na_2O varied from 0.05 to 0.09, then to 0.15.

Solids obtained from each reaction were separated from mother solution and washed with distilled water up to $pH \approx 10$, and dried at $100^\circ C$. Structures of the crystalline products obtained were determined by XRD. Lattice parameter (a_0) was calculated using an internal standard according to the method described by Klug and Alexander (1959). The results obtained are listed in Tables 2 and 3. Morphology of the particles was detected by scanning electron microscope (SEM).

Table 2. Results obtained when the K_2O/Na_2O ratio was fixed at 0.09 and by varying the initial SiO_2/Al_2O_3

Time (week)	SiO_2/Al_2O_3	Type of zeolite crystallization	(a_0)=Å
1	1.5	Amorphous	
2		Amorphous	
3		Amorphous	
4		A+X	
5		A+X	
1	2.6	Amorphous	
2		Amorphous	
3		A+X	
4		A+X	
5		A+X	
1	2.9	Amorphous	
2		Amorphous	
3		Amorphous	
4		X	2.4991
5		X	2.4852

Table 3. Results obtained when the SiO_2/Al_2O_3 ratio was fixed at 2.6 and by varying the initial K_2O/Na_2O

Time (week)	K_2O/Na_2O	Type of zeolite crystallization	(a_0)=Å
1	0.05	Amorphous	
2		Amorphous	
3		Amorphous	
4		A+X	
5		A+X	
1	0.09	Amorphous	
2		Amorphous	
3		A+X	
4		A+X	
5		A+X	
1	0.15	Amorphous	
2		Amorphous	
3		Amorphous	
4		X	2.5019
5		X	2.5032

The effect of increasing SiO_2/Al_2O_3 ratio in the synthesis of zeolite X leads to selectivity with regard to the type of zeolite obtained and to change of lattice

parameter. At $SiO_2/Al_2O_3=1.5$ the co-crystallization of zeolite A+X is obtained after 4 weeks. The zeolite-X proportion is very small. (Fig. 2). At $SiO_2/Al_2O_3=2.6$ the cocrystallization of zeolite A+X is also obtained after 3 weeks. However, the proportion of zeolite X is relatively high compared to the first series. At $SiO_2/Al_2O_3=2.9$, the zeolite X is obtained after 4 weeks (Fig. 2), its lattice parameter $a_0=2.4991\text{Å}$. These results suggested that the critical molar ratio of SiO_2/Al_2O_3 is needed to give individual zeolite X with a minimum reaction time.

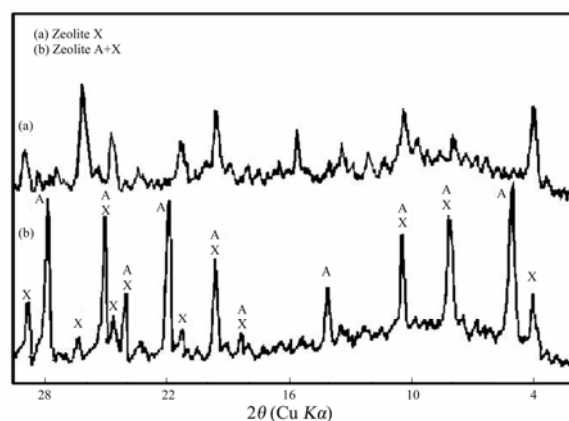


Fig. 2. X-ray diffraction patterns of (a) individual zeolite X; (b) co-crystallization of zeolite A+X.

The effect of replacing sodium ion by potassium ion in synthesis of zeolite X was studied by varying time (1–5 weeks) and keeping SiO_2/Al_2O_3 ratio constant (=2.6), the results obtained are listed in Table 3. It was observed that at low potassium concentrations, the co-crystallization of zeolite A+X was obtained. After four weeks, the proportions of zeolite X increased with increasing potassium content. In the case of $K_2O/Na_2O=0.16$, the individual zeolite X was obtained after 4 weeks of hydrothermal treatment. These results revealed that the critical molar ratio of K_2O/Na_2O is needed to give individual zeolite X with minimum reaction time. After 4 weeks, the zeolite-X was obtained with $a_0=2.5019\text{Å}$; while after 5 weeks a_0 becomes 2.5032Å , revealing an increase in lattice parameter for zeolite X with increasing time of reaction.

The particle size analysis of the two courses of zeolite X with increasing particle size of the second course (at $K_2O/Na_2O=0.15$) reveals the role of potassium ion in the formation of zeolite X. Figure 3 shows that SEM micrographs of final products of the two courses of reaction (Fig. 3a, b) show that the crystal morphology of the co-crystallization of zeolite A+X obtained depends on the concentrations of SiO_2/Al_2O_3 , while zeolite-X is shown in Fig. 3c, d.

The surface area of zeolite-X was measured us-

ing a BET Micromeritics surface area analyzer. The average surface area of zeolite X was about $668 \text{ m}^2 \cdot \text{g}^{-1}$, compared with the literature value of $718 \text{ m}^2 \cdot \text{g}^{-1}$ (Akolekar et al., 1997). This lower value was perhaps to blockage of zeolite pores by non-reacted material or to the fact that zeolite crystals are surrounded by a matrix of unconverted kaolin. The surface area obtained for zeolite A shows a relatively low value ($329 \text{ m}^2 \cdot \text{g}^{-1}$) compared to zeolite X. These observations also provide further evidence for the differences in pore structure of the synthesized zeolites.

In general, the preparation LSX zeolite from kaolin is based on conversion of kaolin to more reactive thermal activated kaolin (calcined kaolin), which is amorphous and much more reactive than the starting material, the exposure of a high surface area of the

calcined kaoline for alkali attack, converted thermal activated kaolin to zeolite-X. This conversion occurs in two distinct stages. At the first stage, there is rapid (complete within two weeks) conversion of thermal activated kaolin (calcined kaolin) to an aluminosilicate phase, which may be described as a gel. During the second stage, crystal growth of zeolite occurs, with increasing reaction time the number of crystals increases. Initially, the process of zeolite-A formation is faster, but then ceases. Individual zeolite-X growth occurs (after 4 weeks). The preferred formation of individual zeolite X may be attributed to the slower nucleation and growth rates by partial replacement of sodium by potassium in the formulation of the initial reaction mixture (Coe et al., 1988).

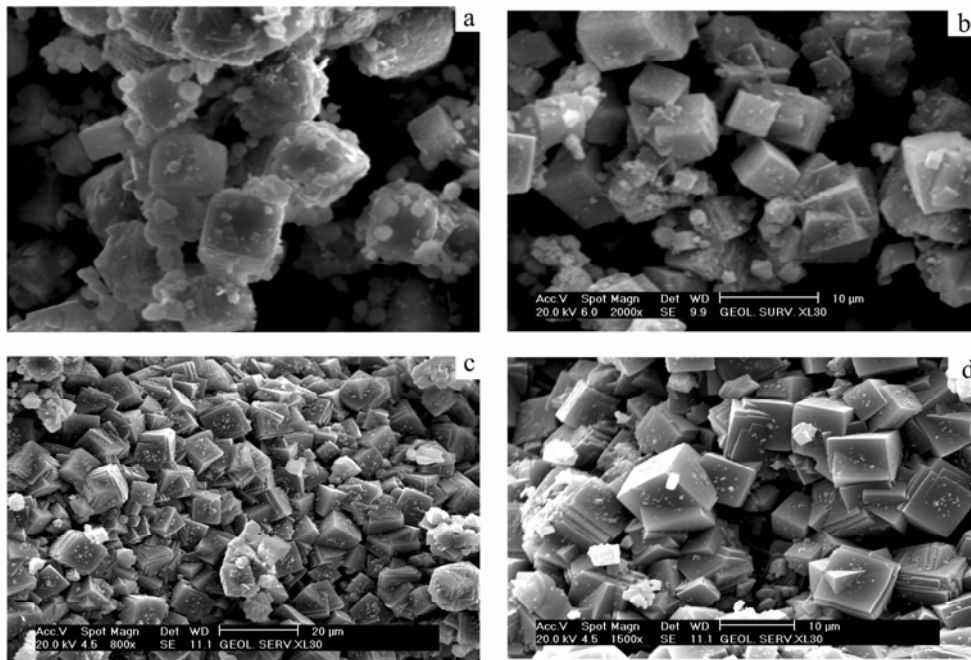


Fig. 3a. Scanning electron micrographs, showing co-crystallization of zeolite A+X, of the first course (a) with low contents of zeolite X; (b) with high contents of zeolite X. Fig. 3b. Scanning electron micrographs, showing individual zeolite X crystals under different magnifications (c and d).

4 Evaluation of the adsorption capacity of the produced zeolite

Zeolites are widely known for their ion exchange properties (Gianneto et al., 2000). The Si/Al framework ratio of the zeolite determines its maximum ion exchange capacity; however, the real capacity may be lower if a proportion of the charge compensation cations are inaccessible for the exchanging ion (Cheetan and Day, 1992). Zinc(II) is relatively large in hydrated ionic radius, and its exchange in zeolitic materials requires a favorable pore opening. The study of the Zn(II) adsorption on zeolite is interesting from an

environmental point of view, and the use of zeolitic materials in the control of pollution has received increasing attention (Petrus and Warchol, 2003).

4.1 Effect of contact time

Figure 4 shows the variation of removal of zinc(II) with contact time for zeolite A, zeolite A+X and zeolite X, respectively. It was observed that the maximum concentration of zinc adsorbed by zeolite X was attained within 30 minutes and about 40 minutes for zeolite A and there after it almost remained static for both. So 40 minutes were fixed as the period of contact time for further studies.

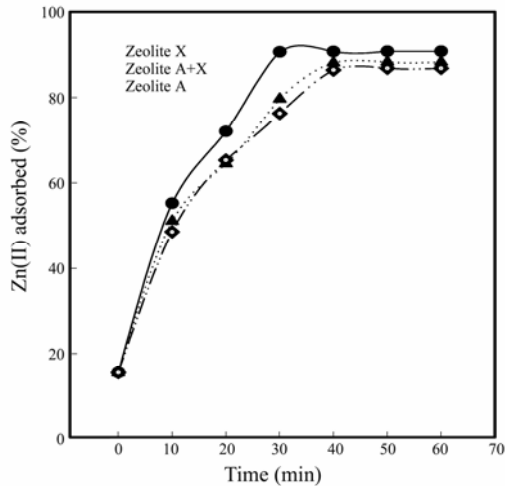


Fig. 4. The relationship between contact time (minute) and Zn(II) adsorption (%) of the obtained zeolites.

4.2 Effect of dosage

In order to fix the minimum dosage for maximum zinc(II) removal, experiments as a function of dosage were carried out. The percent removal of zeolite A, zeolite A+X and zeolite X, respectively at different dosages (0.5–5 g) was measured. It was observed as shown in Fig. 5 that the percent removal increases with increasing sorbent dosage from 0.5 to 2.5 g for zeolite X, and stayed almost constant after 2.5 g. While for zeolite A the percent of removal increases with increasing sorbent dosage from 0.5 to 4 g and stayed almost constant after 4 g. Hence for further experiments the sorbent dosage was optimized as 4 g.

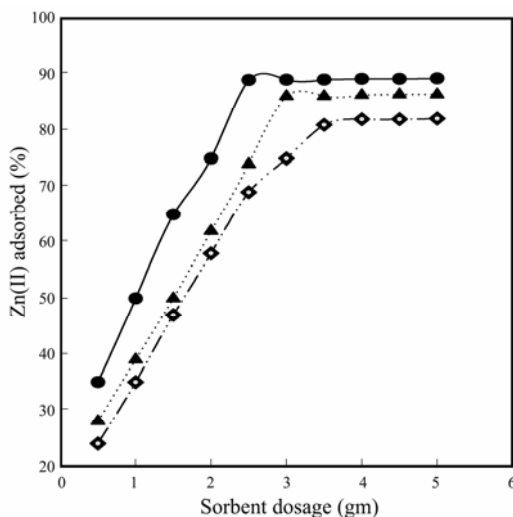


Fig. 5. The relationship between sorbent dosage (gm) and Zn(II) adsorption (%) for the obtained zeolites.

4.3 Effect of pH

The removal of zinc ions from aqueous solution was highly dependent on the solution pH in many

cases as it altered the surface charge on the sorbents (Meenakshi et al., 1991; Lund et al., 2008). In zeolite aqueous systems the potential of surface is determined by the activity of ions (H^+ or OH^-) which react with the mineral surface. As such pH plays an important role in controlling the adsorption of zinc at the zeolite-solution interface. Such interface on acid-base dissociation develops positive and negative charges of the surface (Worrl, 1968; Meenakshi and Viswanathan, 2007). Studies of zinc(II) removal were carried out with zeolite A, zeolite A+X and zeolite X, respectively at various pH values ranging from 4 to 11. The plot of removal of zinc(II) at various pH ranges as given in Fig. 6 clearly indicates that the removal of zinc for zeolite A, zeolite A+X and zeolite X, respectively was influenced by pH of the medium. The removal of zinc of the sorbents was found to be more at lower pH than at higher pH levels. It was found that the higher zinc removal (about 89.1%) was noticed at pH 4 and the efficiency decreased with increasing pH. At neutral pH the capacity being 73.2% and at pH 11 it was only about 65.1% for zeolite X, whereas in zeolite A maximum zinc removal noted at pH 4 was about 86.6%.

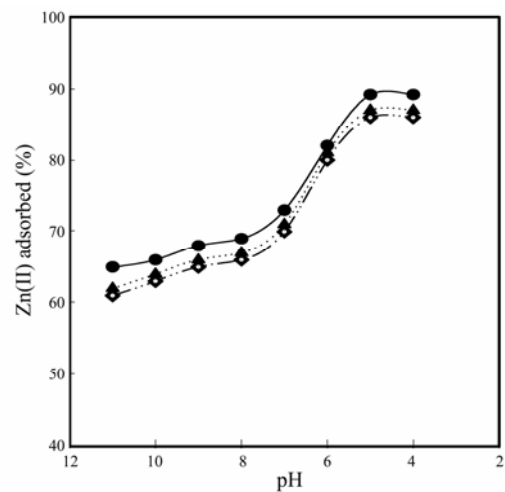


Fig. 6. The relationship between pH and Zn(II) adsorption capacity of the obtained zeolites.

4.4 Effect of the zeolite types

The focus of the present study is also put on evaluating effectiveness of the synthetic zeolite A, zeolite A+X and zeolite X, respectively for removal of zinc(II) from water at pH=4, sorbent dosage 4 g and contact time of 40 min. An aqueous solution (60 mL) containing dissolved zinc(II) (100 to 1000 mg/L zinc) was mixed with the zeolite sample in a bottle and kept on a shaker at room temperature. The zinc removal range from 99.1% for solution containing 100 mg/L zinc(II) to 71.7% for solution containing 1000 mg/L zinc(II), for zeolite X. For zeolite A+X, zinc removal

range from 96.1% for solution containing 100 mg/L zinc(II) to 68.4% for solution containing 1000 mg/L zinc(II). While zeolite A, zinc removal range from 93.3% for solution containing 100 mg/L zinc(II) to 60.4% for solution containing 1000 mg/L zinc(II) (Fig. 7). It is known that the maximum ion exchange capacity of the zeolite depends on the number of cation exchange sites, which is determined by the framework Si/Al ratio. However, it was found that, the zeolite pore opening plays an important role in determining the actual cations exchange of the zeolite (Covarrubias et al., 2007).

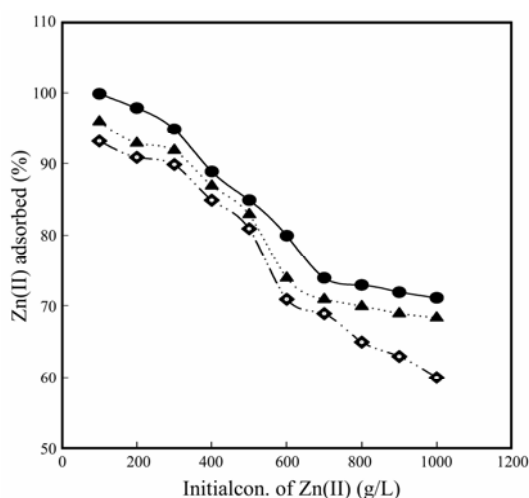


Fig. 7. The relationship between Zn(II) concentrations (g/L) and Zn(II) adsorption capacity of the obtained zeolites.

Zeolite-A possesses a relatively high cation population due to its low Si/Al ratio (~1.0) (Covarrubias et al., 2007). On the other hand, zeolite-X has a lower Si/Al ratio and thereby this zeolite exhibits a higher cation exchange capacity compared with zeolite A. However, the presence of zeolite P in synthesis products decreases the Zn(II) exchange values (Covarrubias et al., 2007). Zeolite-P possesses a higher Si/Al (1.5–2.5) framework ratio than both zeolite-A and zeolite X, and thereby exhibits a lower cation exchange value. Therefore, the cation exchange of the synthetic products is affected by the presence of another zeolite phase as well as the amorphous phase fraction that may be formed during synthesis processes (Covarrubias et al., 2007).

5 Conclusions

It has been found that by using initial SiO₂/Al₂O₃ ratio at 2.9 and fixed K₂O/Na₂O ratio at 0.09, it is possible to avoid co-crystallization of zeolite A+X, where the individual zeolite X was obtained, with lattice parameter (a_0)=2.4991Å. On the other hand, individual zeolite X was also obtained by using K₂O/Na₂O ratio at 0.05 and fixed SiO₂/Al₂O₃ ratio at

2.6, with (a_0)=2.502Å. In both courses the individual zeolite X was obtained after 4 weeks. These suggested the critical molar ratios of both SiO₂/Al₂O₃ and K₂O/Na₂O are needed to give individual zeolite X with minimum reaction time. The particle size of zeolite X increases with increasing potassium content, surface areas of zeolite X obtained are 648 m² · g⁻¹ for the first course, and 688 m² · g⁻¹ for the second course, with an average of about 668 m² · g⁻¹, while it is about (329 m² · g⁻¹) of zeolite A.

The Zn(II) adsorption capacity of synthetic products was determined by the types of zeolite. It was found that the highest zinc exchange was obtained for synthetic zeolite X. The zinc adsorption on zeolite X is favored by the larger pore opening, which facilitates the diffusion of large hydrated zinc ions into the internal cation exchange sites. The presence of other zeolite phases (A or P), as well as the amorphous phase fraction that may be formed during synthesis processes, will affect the zinc exchange capacity. These results show that the synthesized materials are promising for Zn(II) removal from industrial wastewaters.

References

- Akolekar D., Chaffee A., and Howe R.F. (1997) The transformation of kaolin to low-silica X zeolite [J]. *Zeolite*. **19**, 359–365.
- Basaldella E.I. and Tara J.C. (1995) synthesis of LSX zeolite in the Na/K system: Influence of the Na/K ratio. In *Zeolite* [M]. Elsevier Science. **15**, 243–246.
- Chandrasekhar S. and Pramada P.N. (1999) Investigation on the Synthesis of Zeolite NaX from Kerala Kaolin [J]. *J. Porous Materials*. **6**, 283–297.
- Chandrasekhar S. and Pramada P.N. (2008) Microwave assisted synthesis of zeolite A from metakaolin [J]. *Microporous and Mesoporous Materials*. **108** (issues 1–3), 152–161.
- Cheetan A. and Day A. (1992) *Solid State Chemistry Compounds* [M]. pp.266. Oxford University Press Inc., New York.
- Coe C.C., Kuzniak S.M., Srinivasan R., and Jenkins R.J. (1988) In *Perspectives in Molecular Sieves Science* (eds. Flank W.H. and Whyte T.E.) [M]. pp.478. ACS Symp. Ser 368. Am Chem. Soc. Washington, DC.
- Covarrubias C., Garcý'a R., Arriagada R., Ya'nez J., and Garland M. (2007) Cr(III) exchange on zeolite obtained from kaolin and natural mordenite [J]. *Microporous and Mesoporous Materials*. **88**, 220–231.
- Dwyer J. (1984) *Chemistry and Industry* [M]. pp.258–269.
- Elena I., Basaldella E.I., Kikot A., and Tara J.C. (1995) Effect of pellet pore size and synthesis conditions in the *in-situ* synthesis of LSX, Ind [J]. *Eng. Chem. Res.* **34**, 1990–1992.
- El Badry O., Hasssan M., and El Shimi A. (1981) *Contribution to Geochemistry of Some Claystones and Kaolinites of Kalabsha, Egypt* [C]. ICSOBA-AIM Conference Cagliari Italy. No.16, 325–332.
- Falamaki C., Afaran M.S., and Aghaie A. (2006) *In-situ* crystallization of highly oriented silicalite films on porous zircon supports [J]. *J. Am. Ceramic Society*. **89**, 408–414.
- Gianneto G., Montes A., and Rodrý'guez G. (2000) Zeolitas Caracterý'sticas,

- Propiedades y Aplicaciones Industriales, Innovación Tecnológica, Facultad de Ingeniería—UCV, Caracas, p.305.
- Gualtieri A., Norby P., Artoli G., and Hanson J. (1997) Kinetics of formation of Zeolite Na-A (LTA) from nature kaolinites [J]. *Physics and Chemistry of Minerals*. **24**, 191–199.
- Hassan M.S., Ismael I.S., and Ibrahiml A. (2002) Synthesis of zeolite Al-Na from low-grade Kalabsha kaolin [J]. *Journal of Mining, Processing, Metallurgical, Recycling and Environmental Technology, Erzmetall*. **55**(9), 489–494.
- Ichiura H., Okamura N., Kitaoka T., and Tanaka H. (2001) Preparation of zeolite sheet using a papermaking technique Part II The strength of zeolite sheet and its hygroscopic characteristics [J]. *J. Material Science*. **36**, 4921–4926.
- Jiménez A.F., MonzóM., Vicent M., Barba A., and Palomo A. (2008) Alkaline activation of metakaolin-fly ash mixtures: Obtain of zeoceramics and zeocements [J]. *Microporous and Mesoporous Materials*. **108** (issues 1–3), 41–49.
- Klug P.H. and Alexander L.E. (1959) X-ray diffraction procedures (2nd edition) [M]. pp.716. Wiley, New York.
- Lund T., Koretsky C., Landry C., Schaller M., and Das S. (2008) Surface complexation modeling of Cu(II) adsorption on mixtures of hydrous ferric oxide and kaolinite [J]. *Geochemical Transactions*. **9**:9 doi:10.1186/1467-4866-9-9.
- Meenakshi S., Pius A., Karthikeyan G., and Appa Rao B.V. (1991) The pH dependence of efficiency of activated alumina in defluoridation of water, Indian [J]. *J. Environ. Protect*. **11**, 511–513.
- Meenakshi S. and Viswanathan N. (2007) Identification of selective ion-exchange resin for fluoride sorption [J]. *Journal of Colloidal and Interface Science*. **308**, 438–450.
- Mirfendereski S.M., Daneshpour R., and Mohammadi T. (2006) Synthesis and characterization of T-type zeolite membrane on a porous mullite tube [J]. *Desalination*. **200**, 77–79.
- Nah I., Hwang K., Jeonq C., and Choi H.B. (2006) Removal of Pb ion from water by magnetically modified zeolite [J]. *Minerals Engineering*. **19**, 1452–1455.
- Petrus R. and Warchol R. (2003) Micropor [J]. *Mesopor. Mater*. **61**, 137.
- Rollman L.D. and Valyocisk E.W. (1981) *Inorganic Synthesis* [M]. Jhon Wiley and Sons, New York. **22**, 61.
- Roque R., Malherbe A., Valle M.W., Marquez F., Duconge J., and Goosen M.F.A. (2006) Synthesis and characterization of zeolite based porous ceramic membranes [J]. *Separation Science and Technology*. **41**, 73–96.
- Said R. and Mansour A.O. (1971) The discovery of a new kaolin deposits in Wadi Kaslabsha, Nubia, Egypt [J]. *Geol. Surv. & Min. Auth. Rept. No.* 54.
- Shata S. (1991) *Origin of Some Kaolin Deposits in West Central Sinai* [D]. pp.180. M. Sc. Faculty of Science, Suez Canal Univ.
- Tatic M. and Drzaj B. (1985) In *Zeolite* [M]. pp.129. Elsevier Science Publisher B.V., Yugoslavia.
- Wang S.B., Li H.T., and Xu L.Y. (2006) Application of zeolite MCM-22 for basic dye removal from wastewater [J]. *Journal of Colloid and Interface Science*. **295**, 71–78.
- Worrl W.E. (1968) *Textbook of Clays: Their Nature, Origin and General Properties* [M]. Macharen and Sons, London.